

CMOS APS crosstalk characterization via a unique Sub-micron Scanning System

Igor Shcherback, Orly Yadid-Pecht, Senior Member, IEEE,
The VLSI Systems Center
Ben Gurion University
P.O.B. 653 Beer-Sheva 84105, ISRAEL
Tel: 972-8-6461512
Fax: 972-8-6477620
E-Mail: oyp@ee.bgu.ac.il

Abstract

This brief introduces a novel way for CMOS APS crosstalk (CTK) determination and prediction based on our unique Sub-micron Scanning System (SSS) measurements. It enables the crosstalk magnitude determination, the tracking of its main causes, and can be used as a predictive tool for design optimization.

A pronounced crosstalk asymmetry within the array which was revealed by the measurements is analyzed and modeled. The result points out that CMOS APS crosstalk is mostly affected by the specific pixel architecture and the pixels arrangement within the array.

Index terms - CMOS Active Pixel Sensor (APS), Point spread Function (PSF), crosstalk (CTK), diffusion process, modeling.

I. Introduction

This work reports on the pioneer use of our unique sub-micron scanning system (SSS) for diffusion/crosstalk measurements and characterization of focal plane CMOS APS arrays.

In CMOS APS [1-9] the pixel area is constructed of two functional parts: the sensing element itself (the photodiode in a silicon substrate), that has a certain geometrical shape, and the control circuitry required for readout. Electrical crosstalk is the phenomenon whereby photogenerated minority charge carriers generated within the nominal absorption/collection regions of a particular pixel undergo diffusion within the silicon substrate and are collected by a different pixel [10-15]. Pixel signal output is proportional to the product of the integrated photocarriers and the conversion gain. The pixel photosignal dependence on its geometrical shape (the photodiode active area and perimeter), that has been presented in

[16], enables behavior identification of different pixel types and quantifies the device geometry deviations effect on its overall performance.

In this work we propose a technique that allows a unique recording of the internal device behavior. It provides better understanding of the CTK limits in APS arrays and can enable better optimization of pixel design and imager performance.

II. The SSS system and CTK determination - experiment description

The SSS allows the combination of near-field optical and atomic force microscopy (AFM) techniques with standard electrical measurements and enables full point spread function (PSF) extraction for imagers via sub-micron spot light stimulation. This is unique to our system. It is capable to hit onto a well-defined point within the scanning area and focus the incoming parallel light (transferred through the confocal fiber tip, controlled by the AFM system) onto a spot of a desirable diameter size (e.g., $d \leq 0.5 \mu m$ or $d \leq 0.35 \mu m$ according to the technology), after penetration through the transparent oxide (of a certain depth, see Fig. 1). The AFM system also enables a constant spot size during the scan. An optical spot of diameter size $\approx 0.5 \mu m$ was used to scan the APS over a single pixel and its immediate and second step neighbors in a raster fashion scan. A set of measurements for a number of randomly chosen APS chips ($14.4 \times 14.4 \mu m^2$ pitch, L-shaped active photodiode with 53.7% fill factor) fabricated via HP in a standard $0.5 \mu m$ CMOS technology process was performed at the same conditions. The data acquisition was taken at the particular pixel within a $70 \times 70 \mu m^2$ scanned area, i.e., only one pixel was read out at each point of the scan. The obtained signal as a function of the spot position (see Fig. 2) provides a responsivity map of the scanned area that includes the pixel response and the crosstalk influence.

Fig. 1

Fig. 2.

After integration and averaging over the pixel area (for the active pixel and its nearest and second step neighbors), the CTK is determined as the ratio between the active pixel output and one of its neighbors output. The summarized crosstalk results, the discussion and conclusions are presented in the following sections.

III. Crosstalk results - analysis and modeling

The obtained results show that there is an essential difference in the overall CTK obtained from each of the neighbors, i.e., the distribution of the values for the adjacent pixels is as presented in Fig. 2, where the numbers indicate the position in the queue of the overall CTK result in relation to the others. Thus, the signal value obtained from the right nearest neighbor is the highest one, the upper pixel contributes the second highest result, etc.

We have found and show here that the crosstalk has a strong dependence on the particular pixel layout design. We make use of the fact that the generated overall signal is proportional to the pixel geometry [16] and could be presented as the sum of the main, i.e., the photodiode contribution itself, and the periphery contribution, due to the successfully collected diffusion carriers. In the simple case of CTK measurements the output signal depends only on the diffusion contribution, in view of the fact that the readout pixel is not illuminated while CTK is measured from its neighbor. In general, the output signal (from the readout pixel) is proportional to the lateral collecting area, the number of possible contributors, and to the distance that the carrier has to pass before it is collected by the photodiode :

$$V_{out} \propto Pd \cdot (S - A) \cdot \left(\exp\left(-\frac{r}{L_{diff}}\right) \right) \quad (1)$$

The pixel output voltage signal is $V_{out}(I)$ [volt]. Here, Pd [mm^2]- represents the lateral depletion area. $(S - A)$ [mm^2]- represents the unoccupied photodiode surroundings area within the pixel, whereas A [mm^2]- is the photodiode active area, and S [mm^2] - is the pixel area. $\left(\exp\left(-\frac{r}{L_{diff}}\right) \right)$ - represents the one-dimensional diffusion equation solution and indicates the approximated distance r [mm] that the prospective contributor has to pass before it is trapped, L_{diff} [mm]- is the characteristic diffusion length.

The obtained signal map enables easy determination of the distance r [mm] from the depletion boundary (of the readout pixel) such that the signal value becomes $1/3e$ smaller than the value of the central pixel (the signal reduces tenfold relatively to the maximum level, and becomes comparable to the background level). This determines the enclosed area of which the diffusion carriers can contribute. In Fig. 3: (a) indicates the lateral distances, where the signal value reduces to $1/3e$ from its maximum value in relation to the central pixel, (b) represents the corresponding layout with the indication of the enclosed areas. The ratio between the output signals can be approximated as the ratio of sums of the

mentioned enclosed areas multiplied by the corresponding lateral collecting surfaces, i.e., since all other parameters in Eq. 1 remains invariable (including the distance $r[mn]$ which is determined from the measurements), Eq. 1 leads to:

$$\frac{V_{k_{out}}(I)}{V_{m_{out}}(I)} = \frac{\sum P_{k_n} A_{k_n}}{\sum P_{m_n} A_{m_n}} \Bigg|_{\substack{k \neq m \\ \text{at the distance where the value is } 1/3e \text{ of max}}} \quad (2)$$

where V_{out} stays for the output signal, P - represents the lateral collecting surface length (the depletion depth is constant, regarding the cross-section), A - represents the enclosed area, i.e., the area that contributes the prospective carriers, k, m - represent the pixels contributing to the CTK in correspondence to Fig. 3; n - represents the amount of the collecting surfaces, e.g., for pixels "1" and "2" $n=3$, while for pixels "3" and "4" $n=1$. This expression makes use of the axiom of additivity of the antithetical events.

Fig. 3.

Based on the above approximation and the layout data we obtain, for example, that the output signals ratio between pixels "2" and "1" (corresponding to Fig. 3) $V_{1_{out}}/V_{2_{out}} = 1.387$, while the measurement result is ~ 1.390 . It should be noted that the surface leakage, and the non-ideal transmission rate of the overlayers are not included in the present analysis and are considered to be second order effects [17].

We affirm thus that the CTK present within the pixel array is mostly caused by the certain pixel architecture and the pixels arrangement within the array. We therefore conclude that a reliable prediction of the CTK in the imager is possible; the proposed method based on the photoresponse model and the SSS exploitation (the PSF use) for CTK measurements enables both its magnitude determination and its main causes discovery, thus enabling design optimization per each potential pixel application.

IV. Summary

In this work a new method for CMOS photodiode crosstalk determination and prediction, based on our unique submicron scanning system measurements and the CMOS APS photosignal model [16] use, is presented. It reveals the CTK dependence on the pixel geometrical shape (the photodiode active area and perimeter) and the pixels arrangement within the array and brings out clearly the possibility of a design enabling minimum CTK, and thus can be used as a predictive tool for design optimization. The proposed model is process dependant, and further research is required for a process-based model [18, 19]. In addition, since this is the first model giving a quantitative value to the substrate

influence, further model enhancements are expected to follow, including the possible application of crosstalk compensation for CMOS APS arrays.

ACKNOWLEDGEMENTS

The authors would like to thank the Israeli Ministry of Trade for supporting this project. In addition, we would like to thank Mr. Alex Belenky for his help in the chip design and Mr. Boris Belotserkovsky for his help with the chip testing.

References

- [1] J. Hyneczek, "BCMD-An improved photosite structure for high-density image sensors," *IEEE Trans. Electron Devices*, vol.38, ED-5, pp. 1011-1020, May 1991.
- [2] K. Matsumoto, I. Takayanagi, T. Nakamura, R. Ohta, "The operation mechanism of a charge modulation device (CMD) image sensor," *IEEE Trans. Electron Devices*, vol. 38, ED-5, pp. 989-998, May 1991.
- [3] O. Yadid-Pecht, R. Ginosar and Y. Shacham-Diamand, "A random access photodiode array for intelligent image capture," *IEEE Trans. Electron Devices*, vol. 38, no. 8, pp. 1772 - 1781, Aug.1991.
- [4] E. R. Fossum, "CMOS Image Sensors: Electronic Camera on A Chip," *IEEE Trans. Electron Devices*, vol. 44, pp. 1689-1698, Oct 1997.
- [5] O. Yadid-Pecht, B. Mansoorian, E. Fossum, B. Pain, "Optimization of active pixel sensor noise and responsivity for scientific applications," *Proc. SPIE/IS&T Sym. on Electronic Imaging: Science and Technology*, San Jose, California, Feb. 1997.
- [6] Mendis, S. Kemeny, R. Gee, B. Pain, C. Staller, Q. Kim and E. Fossum, "CMOS active pixel image sensors for highly integrated imaging systems," *IEEE J. Solid State Circuits*, vol. 32, pp. 187-197, Feb. 1997.
- [7] P. Magnan, A. Gautrand, Y. Degerli, C. Marques, F. Lavernhe, C. Cavadore, F. Corbiere, J. Farre, O. Saint-Pe, M. Tulet, R. Davancens, "Influence of pixel topology on performances of CMOS APS imagers," *Proc. SPIE*, vol. 3965, 2000.
- [8] J. Bogaerts, B. Dierickx, "Total dose effects on CMOS Active Pixel Sensors," *Proc. SPIE*, vol. 3965, pp. 157-167, 2000.
- [9] H. Tian, B. Fowler, A. El-Gamal, "Analysis of temporal noise in CMOS photodiode active pixel sensor," *IEEE J. Solid State Circuits*, vol. 36, pp. 92-100, Jan. 2001.
- [10] M. Blouke, D. Robinson, "A Method for improving the Spatial Resolution of Frontside-Illuminated CCD's," *IEEE Trans. Electron Devices*, vol. 28, pp. 251-256, Mar 1981.
- [11] J. P. Lavine, E. A. Trabka, B. C. Burkey, T. J. Tredwell, E. T. Nelson, C. N. Anagnosopoulos, "Steady-State Photocurrent Collection in Silicon Imaging Devices," *IEEE Trans. Electron Devices*, vol. 30, ED-9, pp. 1123-1134, Sept. 1983.
- [12] D. Kavaldjiev, Z. Ninkov, "Subpixel Sensitivity Map for a Charge Coupled Device sensor," *Optical Engineering*, vol. 37, no. 3, pp. 948-954, Mar. 1998.
- [13] J. S. Lee, R. I. Hornsey, "Photoresponse of photodiode arrays for solid-state image sensors," *J. Vacuum Science & Tech.*, vol. 18, no 2, pp. 621-625, March 2000.
- [14] T. Dutton, T. Lomheim, M. Nelson, "Survey and comparison of focal plane MTF measurement techniques," *Proc. SPIE*, vol. 4486, pp. 219-246, 2001.
- [15] I. Shcherback, O. Yadid-Pecht, "CMOS APS MTF Modeling," *IEEE Trans. Electron Devices*, vol. 48, ED-12, pp. 2710-2715, Dec. 2001.
- [16] I. Shcherback, O. Yadid-Pecht, "Photoresponse analysis and pixel shape optimization for CMOS Active Pixel Sensors," accepted for publication *IEEE Trans. Electron Devices*, special issue on Image Sensors, Jan. 2003.
- [17] D. Ramey, J. T. Boyd, "Computer Simulation of Optical Crosstalk in Linear Imaging Arrays," *J. Quant. Electron*, vol. 17, pp. 553-556, Apr. 1981.

- [18] H. Wong, "Technology and device Scaling Considerations for CMOS Imagers," *IEEE Trans. Electron Devices*, vol. 43, ED-12, pp. 2131-2142, Dec. 1996.
- [19] T. Lule, S. Benthien, H. Keller, F. Mutze, P. Rieve, K. Seibel, M. Sommer, M. Bohm, "Sensitivity of CMOS based imagers and scaling perspectives," *IEEE Trans. Electron Devices*, vol. 47, ED-11, pp. 2710-2722, Nov. 2000.

List of Figures

Fig. 1. Basic pixel layout /cross-section example of an L-shaped active area pixel design.

Fig. 2. Plot example of an actual PSF measured from an "L" active area shaped pixel. The lighter the tint - the stronger the response.

Fig. 3. (a) Indicates the distance from the depletion boundary where the signal value reduces to $1/3e$ from its maximum value in the central pixel (the lighter the tint - the stronger the response); (b) Represents the corresponding layout with the indication of the enclosed areas.

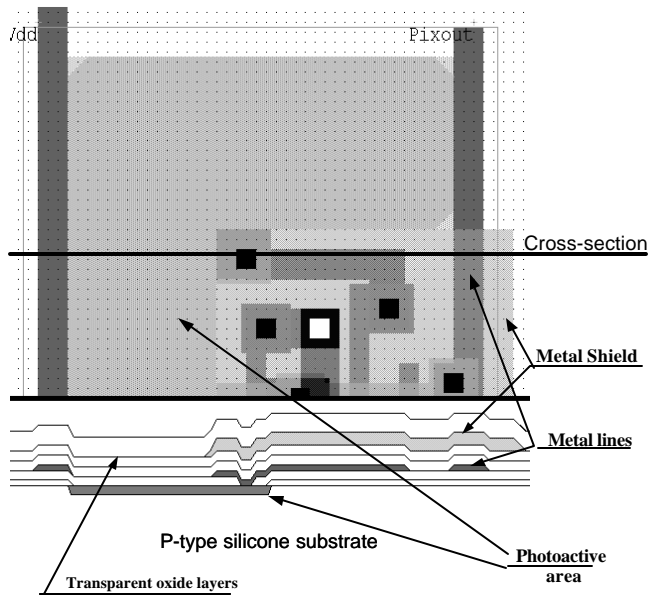


Fig. 1. Basic pixel layout /cross-section example of an L-shaped active area pixel design.

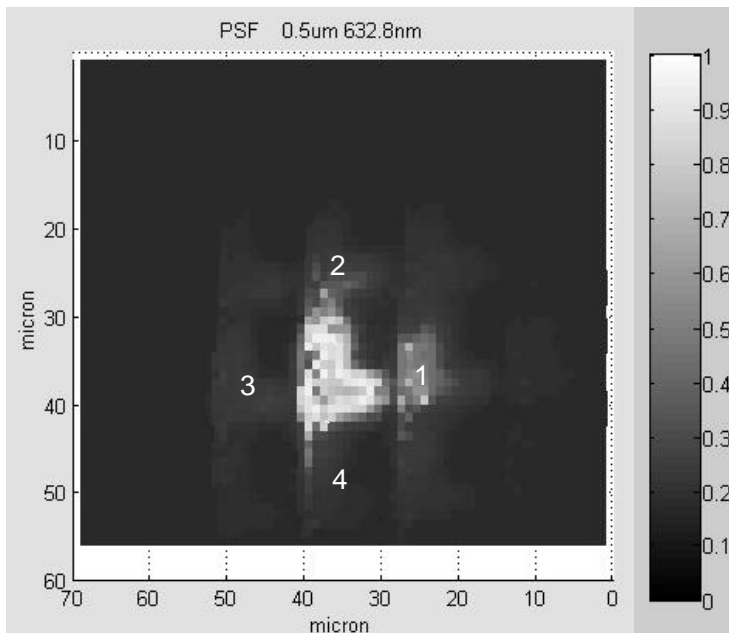


Fig. 2. Plot example of an actual PSF measured from an “L” active area shaped pixel. The lighter the tint - the stronger the response.

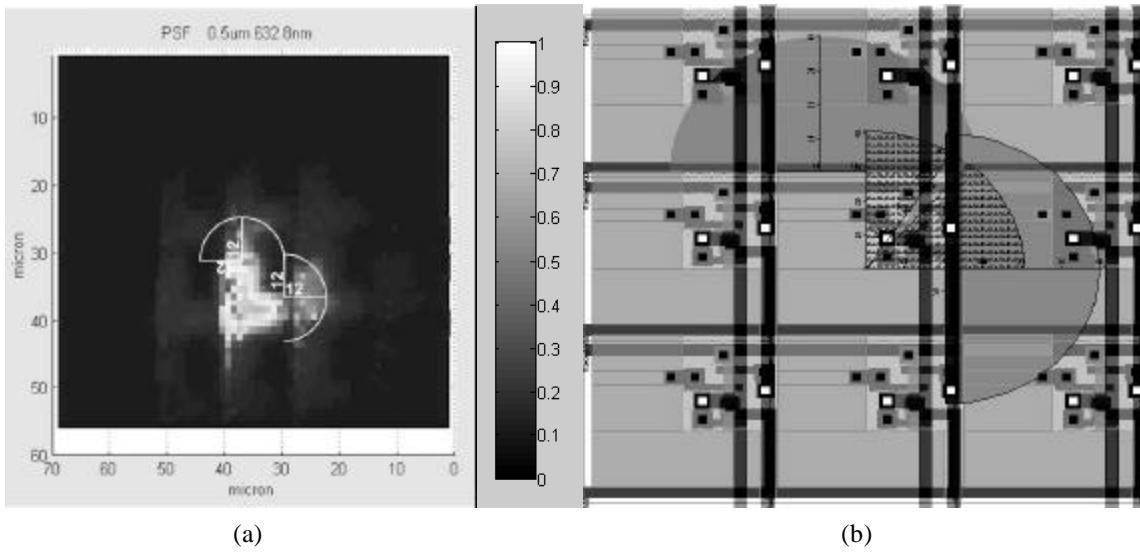


Fig. 3. (a) Indicates the distance from the depletion boundary where the signal value reduces to $1/3e$ from its maximum value in the central pixel (the lighter the tint - the stronger the response); (b) Represents the corresponding layout with the indication of the enclosed areas.